# NEAR SURFACE VELOCITY STRUCTURE OF ANDALUCIA (SOUTHERN SPAIN) AND ALBORAN SEA REGION FROM 0.15-2.0 HZ RAYLEIGH WAVES

**M. Chourak[1], M. Navarro[1], V. Corchete[*1], J. Badal[2]**

[1] Department of Applied Physics, University of Almeria, 04120 Almeria, Spain. *Fax +34 950 015477. e-mail: corchete@ual.es

[2] Department of Theoretical Physics-Geophysics, University of Zaragoza, 50009 Zaragoza, Spain.

## ABSTRACT

A methodology that has been applied for a relatively short time on Seismology is the modelling of very shallow structures from the inversion of dispersion values (group velocity of short period Rg waves). This is possible, because the very short period Rg wave group velocity is sensitive to the variations in the structure of shear velocity for the shallowest layers of the crust. In this line, we have undertaken in the present work, the determination of the shear velocity models for Andalucia and Alboran Sea region (southern Iberia), by means of the generalized inversion of dispersion curves corresponding to Rg waves (short period Rayleigh waves). We use digital filtering techniques, which provide a significant improvement in the signal-to-noise ratio helping to determine a reasonable model for velocity of shear waves. The dispersion curves obtained shows the complexity of the average structure crossing for the waves in each path analysed. We have inverted the average dispersion curves obtained for every path analysed in order to obtain theoretical shear-velocity models, according to the generalized inversion theory. The results obtained show the existence, in the study area, of strong lateral variations in the physical properties of the materials for a rank of depths between 0 to 5 km. The higher velocity values correspond to paths which crossing older structures, whereas the lower values correspond to the paths crossing younger structures.

## KEYWORDS

## RESUMEN

Una metodología que ha sido aplicada desde hace poco tiempo en Sismología, es el modelado de estructuras muy superficiales a partir de la inversión de valores de dispersión (velocidad de grupo de ondas Rg de corto periodo). Esto es posible, debido a que la velocidad de grupo de las ondas Rg de corto periodo, es sensible a las variaciones en la estructura de la velocidad de cizalla de las capas más superficiales de la corteza. En esta línea, nosotros hemos emprendido el presente trabajo: la determinación de los modelos de velocidad de cizalla para la región de Andalucía y mar de Alborán (sur de Iberia), por medio de la inversión generalizada de curvas de dispersión correspondientes a ondas Rg (ondas Rayleigh de periodo corto). Nosotros usamos técnicas de filtrado digital, las cuales proporcionan una significativa mejora en la razón señal-ruido, ayudando a determinar un modelo razonable para la velocidad de las ondas de cizalla. Las curvas de dispersión obtenidas muestran la complejidad de la estructura media cruzada por las ondas en cada trayectoria analizada. Nosotros hemos invertido las curvas de dispersión medias obtenidas para cada trayecto analizado, con el objeto de obtener modelos teóricos de velocidad de cizalla, de acuerdo con la teoría de la inversión generalizada. Los resultados obtenidos muestran la existencia, en el área de estudio, de fuertes variaciones laterales en las propiedades físicas de los materiales dentro de un rango de profundidad que va desde 0 a 5 km. Los valores más altos de velocidad corresponden a trayectos que cruzan las estructuras más antiguas, mientras que los valores más bajos corresponden a trayectorias que cruzan las estructuras más recientes.

## INTRODUCTION

The main objective of this work: the determination of very shallow shear wave velocity structure of Andalucia (southern Spain) and the Alboran Sea, is of much interest for the studies of Seismic Engineering and the Prevention of Seismic Disasters in this region. The short period Rayleigh waves (Rg waves) used in this study to obtain the principal goal described above, constitute part of the answer of the very superficial Earth structure, to the excitation produced by an artificial earthquake (explosion) or a natural earthquake. The knowledge of the velocity of propagation of the short period Rg waves helps to distinguish details of the shallowest structure of the Earth. This relationship between group velocity and frequency (or period) and its lateral change in some region of the Earth are of great importance because it may be correlated with the geologic structure.

In the Iberian area, several studies have showed the existence of some degree of lateral variation in seismic wave velocity and its correlation with the geologic structure. For instance, we have investigated the shallow structure of southern Spain (Almeria region) by means of dispersion analysis of Rg waves generated by blasts or local earthquakes (Navarro et al., 1997), finding continuous velocity distributions with depth of the uppermost crustal layers. We could infer the most conspicuous features of the region in the upper 3.5 km, from the lateral variation in seismic wave velocity, and its correlation with the local geology. Also, in a previous study, Sarrate et al. (1993) studied the shallow crustal structure of another parts of the Iberian Peninsula (the north-west of the Iberian Peninsula), by using dispersion analysis of Rayleigh wave observations. In this study, we carried out a detailed dispersion analysis of high-frequency Rayleigh waves generated by blasts from quarry operations propagated along very short paths. Seismic wave velocity structure of the region was obtained. Retaking this problem for the whole south of Iberia, we obtained the shear velocity structure for a depth range from 0 to 5 km. We will use the inversion process of the dispersion curves in this region (group velocity of the Rg waves for the period ranging between 0.5 to 6 s), like a work tool.

**GEOLOGICAL SETTING**
Before presenting this study we will to locate the reader in the geotectonic situation of the object of this study region. For that reason, previous to the description of this work, we are going to present a brief geologic description of the study zone. With it, we will facilitate the future interpretation of the obtained results, in a geologic frame that the reader can understand. The region under study is located in the southern part of the Iberian Peninsula (see figure 1) and it is composed of several tectonic units that we will describe below.

The *external zone* formed most of the southern part and the minor eastern part of the Iberian Massif, in which during the Mesozoic and part of Cenozoic sediments were accumulated, being deformed and taken off. It is divided in Subbetic and Prebetic and in both exists deposits, generally of marine origin, although the Subbetic presents deeper and therefore harder structures than the Prebetic, which is characterised less by deep sediments (Sanz de Galdeano, 1997). In general, the lithology of the external zone is of type: dolostone, limestones, marls and marl-limestones.

The *complex of the field of Gibraltar* is dominated by alloctones units coming from the basin of the Flyschs, located originally between the internal zones of the Betic Cordillera, the Rift, the Tell and Calabria by a side and the NW of Africa by the south (Wildi, 1983). This unit presents Mesozoics sediments and mainly tertiary turbidites and hemypelagics, which are less compact than the materials of the previous unit.

The *internal zone* is divided tectonically in three superposed complexes and that from top to bottom are: the Maláguide, the Alpujárride and Nevado-Filábride. The Maláguide complex is formed by a Paleozoic basement, whose materials are fundamentally detritics, clays and quartzites, and have a Mesozoic-tertiary cover which are basically formed by dolostone, limestones, marl-limestones, generally very fractured. The Alpujárride complex and Nevado-Filábride present similar stratigraphic sequences of general type: schists, quartzites, gneis, dolostone and limestones, are to say a Paleozoic basement (Kornprobst, 1976) and one Mesozoic or Triassic cover (Priem et al., 1979) carbonated in a part, and both are affected to a certain degree by regional Alpine metamorphism.

The *neogene basins* and the neogene volcanism filled up with sediments of general type: sands, clays, conglomerate and marls, that formed during early Miocene. These neogene basins, formed as much on the internal zone as on the external one or the contact between both. The basins better kept from the Mountain range formed from upper Miocene and are intramountainous basins, like for example the river basins of Almeria, Granada, Guadix-Baza, etc. A rest of volcanism within sediments of early Neogene exist. The volcanism that appears in of Spain (Cabo de Gata and sector of Mazarrón) initiates during Miocene, is especially active in the Tortoniense-Messiniense and arrives at the Pliocene; it extends towards NNE to France and towards SSO to Morocco (Hernández et al., 1987; Sanz de Galdeano, 1990) and is well represented in the Alboran Sea.
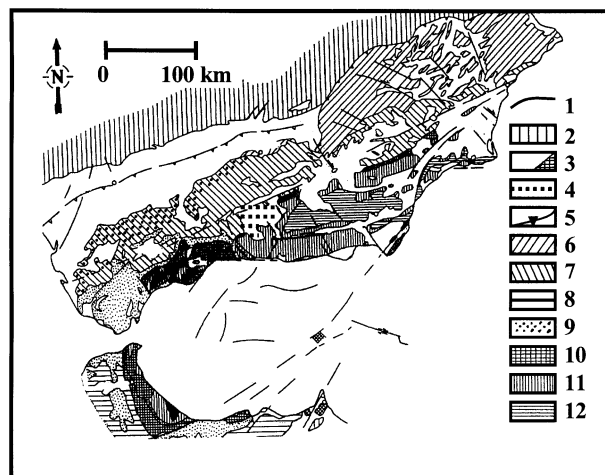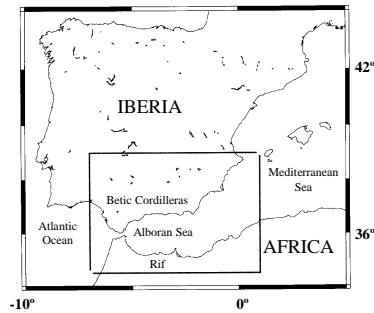
Fig. 1. Upper part: Geographical location of the study area (rectangle) between Iberia and Africa. Lower part: A zoom view of the study zone, emphasising the main structural features and units (after Sanz de Galdeano, 1997). 1: Faults, 2: Foreland, 3: Neogene basins (triangle presents the volcanism), 4: Granada basin, 5: Guadalquivir basin (line present the thrust), 6: Prebetic, 7: Subbetic (small circles present the olistostromes), 8: External zones of the Rif, 9: Flysch, 10: Maláguide and Dorsal, 11: Alpujárride complex, 12: Nevado-Filábride.
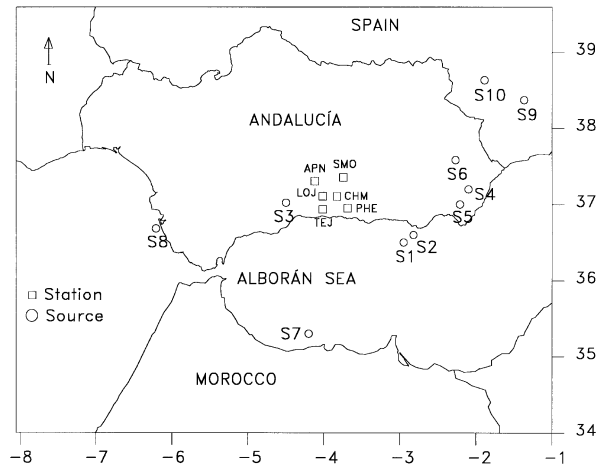
Fig. 2. Locations of sources and stations considered in this study.

Forming western of the Mediterranean, the *Alboran Sea* constitutes a continental basin extended between the South the Iberian Peninsula and the North of Morocco. Of global direction EW, 350 km long and 150 km wide, its waters can reach up to 2000 ms of depth. The marine bottom respectively presents a very complicated frame closely related to the tectonic activity and the regime of sedimentation in this zone (Woodside & Maldonado, 1992; Comas et al., 1992; Docherty & Banda, 1995). The basin of the Alboran Sea formed during lower Miocene and it is characterised fundamentally by clays, sands and marls.

## DATA AND PRELIMINARY ANALYSIS

The Rg wave records used in this study were generated by 43 earthquakes which occurred in the Andalucia and Alboran Sea area during 1990 to 1995 (see table 1), with epicentral distances ranging from 33 to 282 km, approximately, and magnitudes between 2.7 to 4.0 mb. These earthquakes were all recorded by vertical component seismographs of the Regional Seismic Network of Andalucía (RSNA). The study region is covered by the seismic network RSNA managed by the Andalusian Institute of Geophysics (AIG). Codes, coordinates and elevations of the stations used in this study are given in table 3 (and plotted in figure 2). All the events that appear listed in table 1, are grouped around very small areas (source zones). These earthquake epicentres defining 10 source areas are listed in table 2 (and plotted in

*Chourak, M. y colaboradores*

figure 2). Thus, 48 Rg-wave paths between sources and stations has been formed and listed in table 4.

In the preliminary analysis our goal was to analyse the dispersive properties of Rg waves. The result expected in this first step are the epicentre-receiver Rg-wave velocity measurements determinated by means digital filtering of seismograms. After obtaining the ray-path group velocities of the propagating waves, our next goal was to invert the dispersion curves to determine the shear-wave velocity structure (inversion procedure). We use digital filtering techniques (Corchete et al., 1989), which provide a significant improvement in the signal-to-noise ratio helping to determine a reasonable model for velocity of shear waves in the next analysis: the inversion procedure. These operations have, for example, been applied to long-period data by Badal et al. (1996), and to very short-period data by Navarro et al. (1997), showing the effectiveness of the digital filtering for the elimination of noise and other undesirable effects. We used the same filtering process mentioned above with all the selected seismograms.

Table 1. List of seismic events considered in this study.

| Event No | Date (year month day) | | | Origin Time (h-min-s) | Depth (km) | Magnitude (mb) |
|---|---|---|---|---|---|---|
| 1 | 1990 | 09 | 28 | 03:51:37.31 | 6.2 | 3.5 |
| 2 | 1990 | 11 | 03 | 13:53:25.14 | 5.0 | 4.0 |
| 3 | 1990 | 07 | 18 | 19:15:48.36 | 5.0 | 3.8 |
| 4 | 1991 | 04 | 20 | 09:14:09.52 | 0.1 | 3.3 |
| 5 | 1991 | 05 | 06 | 07:25:20.94 | 0.3 | 3.5 |
| 6 | 1991 | 05 | 11 | 20:23:53.72 | 0.1 | 3.3 |
| 7 | 1991 | 10 | 20 | 10:53:50.45 | 0.1 | 3.1 |
| 8 | 1992 | 02 | 24 | 12:20:35.63 | 4.5 | 3.3 |
| 9 | 1992 | 09 | 08 | 12:12:01.66 | 5.0 | 3.0 |
| 10 | 1992 | 11 | 06 | 02:52:46.24 | 2.5 | 3.3 |
| 11 | 1992 | 12 | 17 | 05:01:05.96 | 2.1 | 3.3 |
| 12 | 1993 | 04 | 05 | 01:25:35.88 | 0.4 | 3.4 |
| 13 | 1993 | 12 | 23 | 18:00:08.34 | 4.6 | 4.0 |
| 14 | 1993 | 12 | 27 | 20:01:58.80 | 16.1 | 2.7 |
| 15 | 1994 | 01 | 03 | 01:00:06.88 | 9.9 | 3.9 |
| 16 | 1994 | 01 | 04 | 16:46:46.44 | 3.9 | 3.3 |
| 17 | 1994 | 01 | 04 | 21:08:37.75 | 2.4 | 3.0 |
| 18 | 1994 | 01 | 09 | 16:01:36.34 | 4.4 | 3.4 |
| 19 | 1994 | 01 | 13 | 23:03:03.56 | 2.7 | 2.9 |
| 20 | 1994 | 01 | 16 | 15:55:03.66 | 3.9 | 3.6 |
| 21 | 1994 | 01 | 26 | 16:16:01.66 | 5.0 | 3.0 |
| 22 | 1994 | 02 | 02 | 05:28:05.05 | 7.5 | 3.6 |
| 23 | 1994 | 02 | 02 | 19:09:15.06 | 7.2 | 3.3 |
| 24 | 1994 | 02 | 26 | 07:25:13.99 | 5.2 | 3.6 |
| 25 | 1994 | 03 | 05 | 15:26:06.53 | 7.7 | 3.4 |
| 26 | 1994 | 04 | 20 | 21:23:38.94 | 3.5 | 3.2 |
| 27 | 1994 | 05 | 26 | 14:05:38.86 | 4.5 | 3.1 |
| 28 | 1994 | 05 | 27 | 19:12:52.63 | 5.7 | 3.2 |
| 29 | 1994 | 06 | 07 | 15:32:40.31 | 5.1 | 3.6 |
| 30 | 1994 | 06 | 08 | 03:08:31.14 | 5.4 | 3.6 |
| 31 | 1994 | 06 | 14 | 16:56:30.52 | 5.0 | 3.4 |
| 32 | 1994 | 06 | 15 | 00:15:20.60 | 5.0 | 3.5 |
| 33 | 1994 | 06 | 18 | 03:22:39.87 | 4.8 | 3.2 |
| 34 | 1994 | 06 | 22 | 21:26:29.73 | 5.0 | 3.2 |
| 35 | 1994 | 07 | 24 | 00:45:21.51 | 8.4 | 3.3 |
| 36 | 1994 | 08 | 10 | 20:05:14.03 | 7.9 | 3.2 |
| 37 | 1995 | 02 | 25 | 19:24:25.44 | 8.7 | 3.2 |
| 38 | 1995 | 03 | 18 | 13:40:34.20 | 3.6 | 3.9 |
| 39 | 1995 | 04 | 29 | 07:37:40.84 | 6.1 | 3.2 |
| 40 | 1995 | 06 | 03 | 17:21:25.13 | 4.5 | 3.6 |
| 41 | 1995 | 06 | 07 | 16:20:35.97 | 5.2 | 4.0 |
| 42 | 1995 | 08 | 25 | 19:58:06.92 | 9.0 | 3.2 |
| 43 | 1995 | 11 | 18 | 00:24:47.73 | 9.3 | 3.9 |

*Chourak, M. y colaboradores*

Table 2. Codes and coordinates of the source areas used in this study.

| Sources | Events | Latitude (ºN) | Longitude (ºW) |
|---------|--------|---------------|----------------|
| S1 | 7,9,13,14,15 | 36.50 | 2.95 |
| S2 | 16,17,18,19,20 21,22,23,24,39 | 36.60 | 2.82 |
| S3 | 1,11,25,36,42 | 37.02 | 4.50 |
| S4 | 12,26 | 37.20 | 2.10 |
| S5 | 8,35,37,38,40, 41,43 | 37.00 | 2.21 |
| S6 | 4,5,6 | 37.58 | 2.27 |
| S7 | 27,28,29,30,31, 32,33,34 | 35.30 | 4.20 |
| S8 | 3 | 36.64 | 6.21 |
| S9 | 2 | 38.37 | 1.37 |
| S10 | 10 | 38.63 | 1.89 |

Table 3. Codes, coordinates and elevations of the stations used.

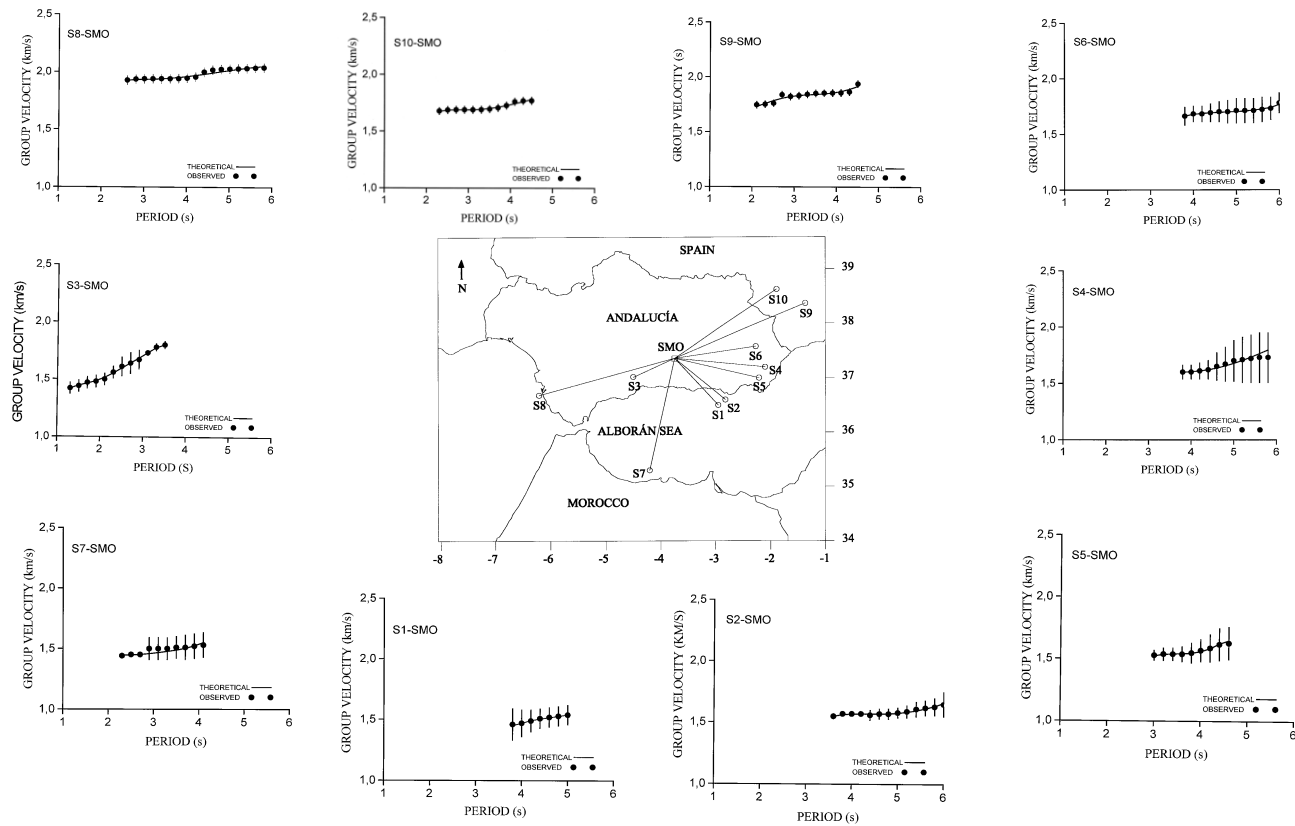| Station | Latitude (ºN) | Longitude (ºW) | Altitude (m) |
|---------|---------------|----------------|--------------|
| PHE | 36.952 | 3.688 | 1360 |
| TEJ | 36.915 | 4.014 | 1480 |
| LOJ | 37.109 | 4.105 | 1340 |
| SMO | 37.358 | 3.743 | 1170 |
| APN | 37.307 | 4.120 | 1160 |
| CHM | 37.105 | 3.829 | 860 |

Fig. 3. Rg wave group velocity dispersion curves measured along all epicentre-receiver paths with SMO station. For every path we can see a comparison between the solution of the forward problem, the theoretical group velocity dispersion curve (continuous line) predicted by the earth model obtained after inversion, and the observed dispersion of group velocity (dots). Vertical bars represent standard deviations (1-sigma errors) at several periods.

*Chourak, M. y colaboradores*

Thus, the group-velocity dispersion curves for all paths are obtained and listed in table 4. The dispersion curves for SMO station have been plotted in figure 3. For each seismic trajectory, both the path-length travelled by the waves and the respective events involved are known (table 4). Figure 3 shows the mean dispersion curves of Rg-wave group velocity measured along every path considered (with SMO station) and the standard deviation (1-sigma errors) plotted with vertical bars at various periods for each case. The dispersion curves obtained show the complexity of the average structure crossed by the waves for each path analysed. Nevertheless, the filtering techniques mentioned above allow us to obtain the group velocity values for each path analysed.

## SHEAR VELOCITY MODELS

With the purpose of obtaining earth models in terms of path-averaged shear-wave velocities, we inverted the average dispersion curves obtained for every path analysed. The standard deviation (1-sigma errors) related to each group velocity dispersion curve, has been provided to account for the estimation of the shear wave velocity uncertainties. We perform inverse modelling by generalized inversion in order to obtain theoretical shear-velocity models according to the inversion theory (Tarantola, 1987).

For all paths considered with SMO station, we also estimated the reliability of the inversion results by means of forward modelling: through a comparison of the theoretical group-velocity dispersion curve predicted by the earth model obtained by inversion, with the observed dispersion data. The theoretical solutions derived by forward modelling and the observed group velocity dispersion, are shown for all paths with SMO station in figure 3, as continuous and dot line, respectively. The shear wave velocity values from inversion of group velocities are shown in table 5, Shear velocity values and group velocity values, shows in general a similar trend.
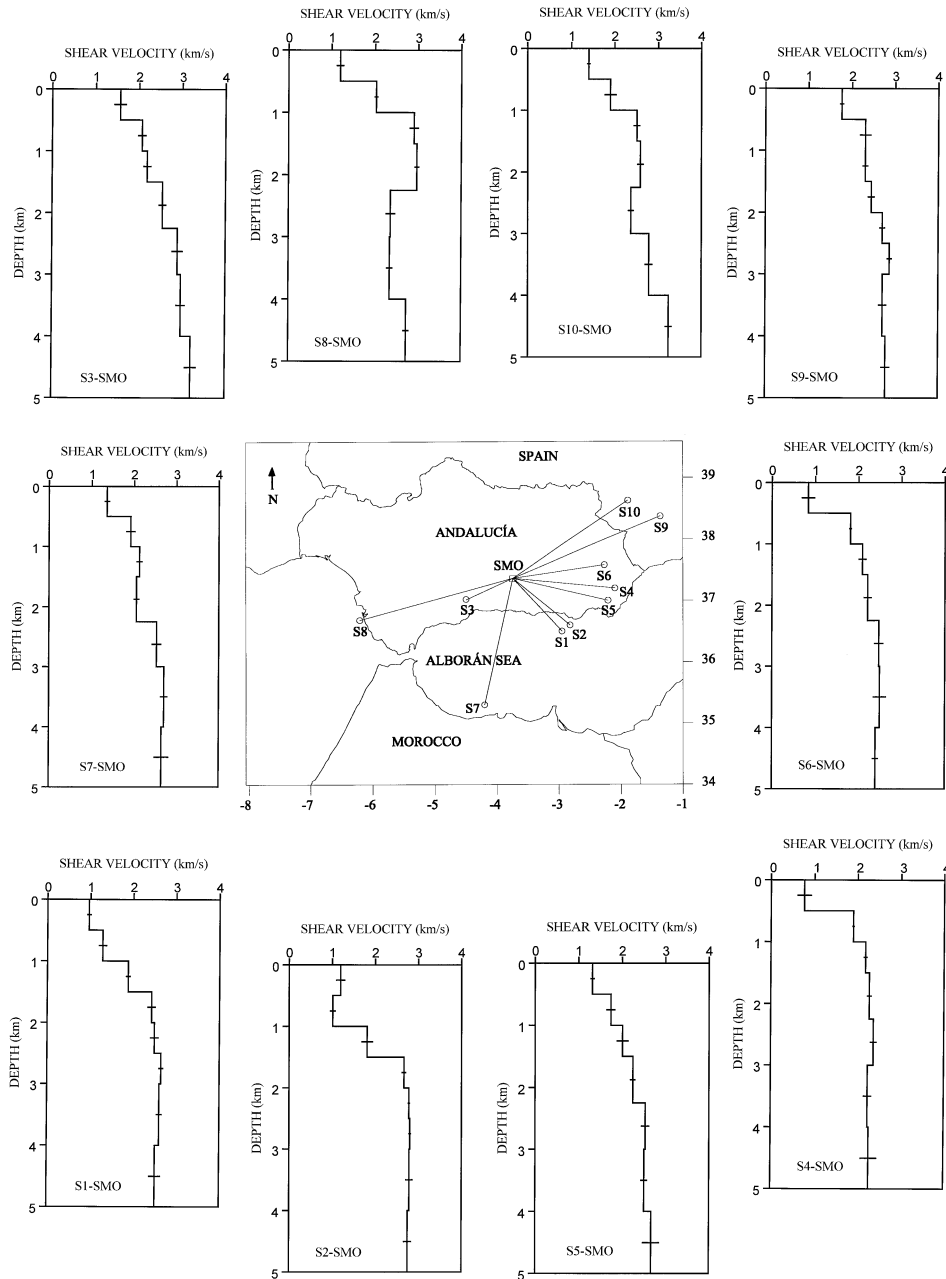
Fig. 4. Shear wave velocity models derived from inversion of ray-path group velocities for the paths with SMO station. Horizontal bars represent standard deviations (1-sigma errors) at several depths.

*Chourak, M. y colaboradores*

## INTERPRETATION AND CONCLUDING REMARKS

In this study we wanted to determine the very superficial elastic structure of Andalucia and the Alborán Sea region, from the inversion of Rg waves dispersion curves generated by local earthquakes registered by the short period seismic stations of the Andalusian Seismic Network. The group velocity values obtained for the Rg waves in the different analyzed paths are between 1.12 and 2.15 km/s for a rank of periods between 0.6 and 6.0 s, obtaining a different dispersion curve for each path analysed. In spite of the structural complexity of the study area, mainly the Eastern part, the group velocity values obtained for each path shows a good correlation with the main features of the area, surrounding the respective path. We found, in general, that the group velocity is greater for the paths contained, total or partially, in the oldest structures.  It is being observed that the paths corresponding to the sources S4, S5, and S6, that crossing the Nevado-Filabride complex, display the highest values of group velocity (between 1.43 and 2.15 km/s, for a rank of periods between 1.6 and 6.0 s). These differences are a consequence of the superficial heterogeneities that affect the propagation of the Rg waves.

The seismic sources S1, S2 and S7 are located in the Alboran Sea and their paths, crossing sedimentary structures, show the lower values of dispersion.  The inversion of the dispersion curves for the differents paths source-station analyzed, has allowed to obtain the elastic model of the structure crossed by each path, each model being the average of the different structures that each path crosses. We observed that the values of shear velocity are in general greater for the paths crossing the oldest structures (Complex Nevado-Filábride, Alpujárride complex and subbetic structure), whereas the lowest values correspond to the paths contained in the sedimentary structures of  the study area. The shear velocity models have been obtained for a rank of depth between 0.0 and 5.0 km.

If we compare the group velocity values and the shear velocity models obtained for the different seismic sources and the SMO station (see figures 3 and 4), we observe that paths S1-SMO and S2-SMO crossing the same geologic structure (formed by neogene-quaternary materials and Alpujárride complex) present similar trends. Shear velocity models have a quite similar trend, with values between 1.00 to 2.80 km/s. The path S3-SMO is contained completely on a subbetic structure, therefore it crosses in average a more rigid structure than the previous one, showing a shear velocity model with values from 1.56 to 3.20 km/s.

Table 4. Source-station paths analysed in this study, the events involved in each case (as listed in table 1) and the average distances travelled by the waves. The fifth column shows the studied range of depth. The sixth shows the number of layers considered in the Earth model. The seventh column shows the shear velocity range, obtained after the inverse process of the dispersion curve for this path. Finally, the last column displays the rank of values for the standard deviation ($1\text{-}\sigma$ error) of the shear velocity for each path.

| Paths | Events | Source-station | Distance (km) | $\Delta z$ (km) | N | $\Delta\beta$ (km/s) | $\Delta\sigma_\beta$ |
|---|---|---|---|---|---|---|---|
| 1 | 7,9,13,14,15 | S1--APN | 118.65 | 0.0-5.0 | 8 | 0.98-2.78 | 0.04-0.13 |
| 2 | 13,14,15 | S1--TEJ | 089.50 | 0.0-5.0 | 11 | 1.11-2.47 | 0.05-0.15 |
| 3 | 7,9,14 | S1--SMO | 107.10 | 0.0-5.0 | 8 | 1.00-2.80 | 0.04-0.10 |
| 4 | 9,13,14,15 | S1--CHM | 84.11 | 0.0-5.0 | 11 | 0.86-2.69 | 0.03-0.14 |
| 5 | 7,9,14 | S1--LOJ | 120.38 | 0.0-5.0 | 8 | 1.00-3.47 | 0.04-0.13 |
| 6 | 13 | S1--PHE | 060.29 | 0.0-5.0 | 8 | 0.96-2.76 | 0.04-0.14 |
| 7 | 16,18,20 | S2--APN | 137.22 | 0.0-5.0 | 7 | 1.21-2.62 | 0.08-0.11 |
| 8 | 16,18,20,23, 39 | S2--CHM | 100.77 | 0.0-5.0 | 8 | 0.98-2.76 | 0.04-0.12 |
| 9 | 17,18,20,21,22,24 | S2--PHE | 083.88 | 0.0-5.0 | 7 | 1.28-2.73 | 0.04-0.11 |
| 10 | 18,21,22,23 | S2--LOJ | 124.41 | 0.0-5.0 | 8 | 1.00-2.84 | 0.05-0.10 |
| 11 | 17,19,21,22 | S2--TEJ | 101.79 | 0.0-5.0 | 7 | 0.95-2.54 | 0.01-0.10 |
| 12 | 18,19,20,23,39 | S2--SMO | 111.00 | 0.0-5.0 | 8 | 1.01-2.80 | 0.02-0.12 |
| 13 | 1,42 | S3--SMO | 067.19 | 0.0-5.0 | 7 | 1.56-3.20 | 0.07-0.13 |
| 14 | 1,11,25,42 | S3--TEJ | 041.66 | 0.0-5.0 | 7 | 1.51-3.03 | 0.05-0.14 |
| 15 | 1,11,25,42 | S3--LOJ | 032.78 | 0.0-5.0 | 7 | 1.85-2.89 | 0.06-0.14 |
| 16 | 1,11,36 | S3--CHM | 059.38 | 0.0-5.0 | 7 | 0.87-2.80 | 0.05-0.12 |
| 17 | 12,26 | S4--LOJ | 175.00 | 0.0-5.0 | 8 | 1.31-2.72 | 0.03-0.09 |
| 18 | 12,26 | S4--CHM | 150.88 | 0.0-5.0 | 8 | 1.70-3.06 | 0.03-0.12 |
| 19 | 12,26 | S4--TEJ | 171.24 | 0.0-5.0 | 8 | 1.16-2.62 | 0.02-0.08 |
| 20 | 12,26 | S4--SMO | 141.59 | 0.0-5.0 | 7 | 0.76-2.37 | 0.01-0.18 |
| 21 | 12,26 | S4--APN | 178.84 | 0.0-5.0 | 8 | 1.40-2.87 | 0.03-0.11 |
| 22 | 37,40,43 | S5--TEJ | 146.68 | 0.0-5.0 | 7 | 1.50-3.04 | 0.03-0.13 |
| 23 | 38,41 | S5--SMO | 140.86 | 0.0-5.0 | 7 | 1.30-2.67 | 0.03-0.18 |
| 24 | 8,35,37 | S5--LOJ | 138.41 | 0.0-5.0 | 7 | 1.41-2.82 | 0.05-0.10 |
| 25 | 8,41 | S5--CHM | 130.94 | 0.0-5.0 | 7 | 1.01-2.54 | 0.03-0.09 |
| 26 | 5,6 | S6--CHM | 148.53 | 0.0-5.0 | 7 | 1.43-2.83 | 0.01-0.09 |
| 27 | 5,6 | S6--TEJ | 166.96 | 0.0-5.0 | 8 | 1.59-3.00 | 0.02-0.16 |
| 28 | 4,5,6 | S6--LOJ | 169.82 | 0.0-5.0 | 7 | 0.96-2.45 | 0.01-0.10 |
| 29 | 4,5,6 | S6--SMO | 131.76 | 0.0-5.0 | 7 | 0.83-2.49 | 0.02-0.14 |
| 30 | 4,5,6 | S6--APN | 165.30 | 0.0-5.0 | 7 | 1.68-2.98 | 0.07-0.15 |
| 31 | 4,5,6 | S6--PHE | 142.84 | 0.0-5.0 | 8 | 1.70-2.98 | 0.03-0.16 |
| 32 | 27,28,29,33,34 | S7--LOJ | 199.02 | 0.0-5.0 | 8 | 0.98-2.78 | 0.04-0.10 |
| 33 | 30,31 | S7--TEJ | 172.22 | 0.0-5.0 | 11 | 1.00-2.85 | 0.02-0.09 |
| 34 | 29,32,34,30 | S7--PHE | 187.33 | 0.0-5.0 | 8 | 0.99-2.75 | 0.03-0.11 |
| 35 | 29,30,33 | S7--CHM | 199.95 | 0.0-5.0 | 7 | 1.47-3.20 | 0.04-0.15 |
| 36 | 29,30,31,34 | S7--SMO | 212.22 | 0.0-5.0 | 7 | 1.35-2.70 | 0.05-0.16 |
| 37 | 28,30,34 | S7--APN | 202.88 | 0.0-5.0 | 7 | 0.71-2.44 | 0.01-0.15 |
| 38 | 3 | S8--APN | 199.57 | 0.0-5.0 | 7 | 0.95-2.48 | 0.03-0.08 |
| 39 | 3 | S8--PHE | 226.35 | 0.0-5.0 | 7 | 1.28-2.86 | 0.02-0.11 |
| 40 | 3 | S8--LOJ | 193.83 | 0.0-5.0 | 7 | 1.00-3.73 | 0.01-0.17 |
| 41 | 3 | S8--CHM | 217.30 | 0.0-0.5 | 8 | 1.88-2.77 | 0.04-0.16 |
| 42 | 3 | S8--SMO | 232.75 | 0.0-5.0 | 7 | 1.19-2.97 | 0.04-0.10 |
| 43 | 3 | S8--TEJ | 197.18 | 0.0-5.0 | 7 | 1.62-3.00 | 0.03-0.12 |
| 44 | 2 | S9--SMO | 235.88 | 0.0-5.0 | 8 | 1.75-2.87 | 0.04-0.12 |
| 45 | 2 | S9--LOJ | 277.23 | 0.0-5.0 | 7 | 1.06-2.83 | 0.03-0.10 |
| 46 | 2 | S9--PHE | 256.57 | 0.0-5.0 | 8 | 1.69-2.84 | 0.04-0.09 |
| 47 | 2 | S9--TEJ | 282.15 | 0.0-5.0 | 8 | 1.39-2.90 | 0.05-0.15 |
| 48 | 10 | S10--SMO | 214.57 | 0.0-5.0 | 7 | 1.39-3.24 | 0.02-0.13 |

*Chourak, M. y colaboradores*

The paths S4-SMO, S5-SMO and S6-SMO which crossing similar geologic structures, are contained mainly in a structure formed by neogene-quaternary and Nevado-Filábride complex. The dispersion curves show similar values for group velocity.

The source S7 corresponds to events of the seismic series of Hoseima (north of Morocco) and the epicentres are in the sea. The paths corresponding to this source are mainly contained in the Alborán Sea basin. The length of the continental part of each path from S7 to the station is different, which produces slight differences in dispersion curves. The lower values of group velocity correspond to the paths with the stations near to the coast (TEJ and PHE) and therefore the continental contribution is small. The highest values correspond to the path S7-APN, which is to 70 % contain in the Alboran Sea basin and to 30% in the Alpujárride and subbetic structure. For this reason velocity values are increased respect to the other paths. The continental part corresponding to path S7-SMO is to 30 % contain in the Alpujárride complex and to 70% on the neogene-quaternary basin (Granada basin). The shear velocity models corresponding to the paths with the source S7 partially characterise the elastic structure of the Alborán Sea region. The paths corresponding to the source S8 are crossing a subbetic structure mainly, and show higher group velocity values than the corresponding ones the paths partially contained in a sedimentary basin.

The path S8-SMO can be completely considered to be contained in a subbetic structure and shows shear velocities from 1.19 to 2.97 km/s, for a rank of depth between 0.0 to 5.0 km. The paths of the sources S9 and S10 to seismic station SMO cross a very complex structure formed by materials of different tectonic units (mainly Subbetic and Prebetic) and sedimentary structures. For this reason we don't find great differences in the group velocities and shear velocity models for both paths.

The results exposed above show the existence, in the study area, of strong lateral variations of the physical properties of the materials for the rank of depth under consideration (0 to 5 km). The group velocity obtained for the different paths analyzed in this study show remarkable differences. The higher velocity values correspond to the paths, which are crossing older structures, whereas the lower values correspond to the paths crossing younger structures.

## REFERENCES

Badal, J., V. Corchete, G. Payo, L. Pujades & J. A. Canas. 1996. Imaging of Shear-wave velocity structure beneath Iberia. Geophys. J. Int., 124, 591-611.

Comas M.C., V. García & M. J. Jurado. 1992. Neogene tectonic evolution of the Alboran sea from MCS data, Geo-Marine Ltters, 12, 157-164.

Corchete, V., J. Badal, G. Payo & F.J. Serón. 1989. Filtrado de ondas sísmicas dispersadas. Rev. de Geofísica, 45, 39-58.

Docherty & Banda. 1995. Evidence for eastward migration of the Alboran sea based on regional subsidence analysis: a case for basin formation by delamination of the subcrustal lithosphere? Tectonics, Vol. 14, Nº 4, pp. 804-818.

Hernández, J., F. D. de Larouziere, Bolze, J. et P. Bordet. 1987. Le magmatisme néogene bético-rifain et le couloir de décrochement trans-Alboran. Bull. Soc. géol. France, Vol. ·, pp. 257-267.

Kornprobst, J. 1976. Signification structurale des péridotites dans l'orogène bético-rifain: arguments tirés de l'étude des détritus observés dans les sédiments paléozoïques. Bull. Soc. géol. France, Vol. 18 (3), pp. 607-618.

Navarro, M., V. Corchete, J. Badal, J. A. Canas, L. Pujades & F. Vidal. 1997. Inversion of Rg waveforms in southern Spain, Bull. Seismol. Soc. Am., 87, 847-865.

Priem, H N A, N A I M Boelrijk, E H Hebeda, I S Oen, E A T Verdurmen & R H Verchure. 1979. Isotopic dating of the emplacement of the ultramfic masses in the Serrania de Ronda, southern Spain. Contributions Mineral. Petrol., Vol. 70, pp. 103-109.

Sanz de Galdeano, C. 1990. Geologic evolution of the Betic Cordilleras in the Western Mediterranean, Miocene To the present. Tectonophysics, Vol. 172, pp. 107-119.

Sanz de Galdeano, C. 1997. La zona interna Bético-Rifeña. Univ. De Granada, Granada, 318 pp.

Sarrate, J., J. A. Canas, L. Pujades, J. Badal, V. Corchete & G. Payo. 1993. Shallow structure of part of northwestern Iberia from short-period Rayleigh-wave observations, Tectonophysics, 221, 95-105.

Tarantola, A. 1987. Inverse Problem Theory. Methods for Data Fitting and Model Parameter Estimation, Elsevier, Amsterdam.

Wildi, W. 1983. La chaîne Tello-Rifaine (Algérie, Maroc., Tunisie): structure, stratigraphie et évolution du trias au Miocène. Rev. Géol. Dyn. Geodr. Phys., Vol. 24, Nº 3, pp. 201-297.

Woodside, J. M. & A. Maldonado. 1992. Styles of compressional neotectonics in the Eastern Alboran Sea, Geo-Mar. Lett., 12, 111-116.